

# Multiobjective optimization approach to shape and topology optimization of plane trusses with various aspect ratios

Makoto Ohsaki<sup>1\*</sup>, Saku Aoyagi<sup>1</sup>, Kazuki Hayashi<sup>1</sup>

Department of Architecture and Architectural Engineering, Kyoto University, Kyoto-Daigaku Katsura, Nishikyo, Kyoto 615-8540, Japan, ohsaki@archi.kyoto-u.ac.jp

## Abstract

A multiobjective optimization method is proposed for obtaining the optimal plane trusses simultaneously for various aspect ratios of the initial ground structure as a set of Pareto optimal solutions generated through a single optimization process. The shape and topology are optimized simultaneously to minimize the compliance under constraint on the total structural volume. The strain energy of each member is divided into components of two coordinate directions on the plane. The force density method is used for alleviating difficulties due to existence of coalescent or melting nodes. It is shown in the numerical example that sufficiently accurate optimal solutions are obtained by comparison with those obtained by the linear weighted sum approach that requires solving a single-objective optimization problem many times.

## Keywords

Topology optimization, Shape optimization, Multiobjective optimization, Truss, Compliance

## 1 Introduction

There have been numerous studies for topology optimization and shape optimization of plane trusses under various static and dynamic constraints. However, there exist several difficulties for simultaneously optimizing the shape and topology of trusses. The simplest approach may be to consider both of the member cross-sectional areas and the nodal coordinates as design variables. However, in this case, structural analysis becomes difficult when coalescent nodes [1] or melting nodes [2] exist, and consequently, the stiffness matrix becomes singular. Since topology optimization often leads to an unstable truss, global stability constraint is one of the important subjects for recent studies on the shape and topology optimization, or layout optimization, of plane trusses [3]. Weldeyesus *et al.* [4] incorporated global stability constraint as well as the bound constraints on the nodal coordinates.

The force density method (FDM) was originally developed for self-equilibrium analysis of tension structures such as cable nets and tensegrity structures [5]. Descamps and Coelho [6] optimized layout of the hanging members of a bridge truss assigning the zero lower bound for the force densities so that all members have tension forces. To prevent the difficulties on simultaneous shape and topology optimization of trusses, Ohsaki and Hayashi [7] proposed a method using the force densities of members as design variables for the problem of minimizing the compliance under constraint on the total structural volume. Existence of extremely short members can be indirectly avoided by assigning appropriate bounds on force densities [8]. In the process of shape and topology optimization of plane trusses, the locations of supports and loaded nodes are generally fixed at those specified by the initial ground structure. However, the optimal load path strongly depends on the ratios of distances among the supports and loaded nodes, which are varied along with the aspect ratio of the initial ground structure. Therefore,

it is beneficial for the engineers if the optimal trusses for various aspect ratios of the ground structure can be found simultaneously by a single optimization process.

Zhang and Ohsaki [9] showed that the self-equilibrium state of tensegrity structures is invariant against affine motions when the equilibrium equations are formulated with respect to the force densities. Utilizing this property, the force densities of members are chosen as design variables in this study. The total strain energy, which is equivalent to a half of the compliance, is divided into two in-plane directional components to formulate the two objective functions of a multiobjective optimization problem, and the optimal solutions for various aspect ratios of the initial ground structure are generated as a set of Pareto optimal solutions using a multiobjective genetic algorithm.

## 2 FDM for simultaneous shape and topology optimization of trusses

In this section, we briefly summarize the results in Ohsaki and Hayashi [7] for completeness of the paper.

Consider an optimization problem of minimizing the compliance under constraint on the total structural volume of a truss. Let  $N_i$  denote the axial force of the  $i$ th member of a truss consisting of  $m$  members. The truss is subjected to a single loading condition, and the force density  $q_i$  is defined as the force divided by the length  $L_i$ , i.e.,

$$q_i = \frac{N_i}{L_i} \quad (i = 1, \dots, m) \quad (1)$$

Let  $\mathbf{Q} \in \mathbb{R}^{n \times n}$  denote the force density matrix constructed from the force densities of members and the connectivity matrix, where  $n$  is the number of nodes including the supports. The equilibrium equations in  $x$ - and  $y$ -directions of a truss have the following forms:

$$\mathbf{Q}\mathbf{x} = \mathbf{p}^x, \quad \mathbf{Q}\mathbf{y} = \mathbf{p}^y \quad (2)$$

where  $\mathbf{x} \in \mathbb{R}^n$  and  $\mathbf{y} \in \mathbb{R}^n$ , respectively, are the vectors of  $x$ - and  $y$ -coordinates of nodes including supports, and  $\mathbf{p}^x \in \mathbb{R}^n$  and  $\mathbf{p}^y \in \mathbb{R}^n$  are the nodal load vectors including the reactions in  $x$ - and  $y$ -directions, respectively, at the supports.

The nodes are classified into free and fixed nodes, which are denoted by the subscripts ‘free’ and ‘fix’, respectively. The components between the free and fixed nodes are denoted with ‘link’. The set of  $x$ - and  $y$ -directional equilibrium equations in (2) are partitioned as

$$\begin{pmatrix} \mathbf{Q}_{\text{free}} & \mathbf{Q}_{\text{link}} \\ \mathbf{Q}_{\text{link}}^T & \mathbf{Q}_{\text{fix}} \end{pmatrix} \begin{pmatrix} \mathbf{x}_{\text{free}} \\ \mathbf{x}_{\text{fix}} \end{pmatrix} = \begin{pmatrix} \mathbf{0} \\ \mathbf{p}_{\text{fix}}^x \end{pmatrix} \quad (3a)$$

$$\begin{pmatrix} \mathbf{Q}_{\text{free}} & \mathbf{Q}_{\text{link}} \\ \mathbf{Q}_{\text{link}}^T & \mathbf{Q}_{\text{fix}} \end{pmatrix} \begin{pmatrix} \mathbf{y}_{\text{free}} \\ \mathbf{y}_{\text{fix}} \end{pmatrix} = \begin{pmatrix} \mathbf{0} \\ \mathbf{p}_{\text{fix}}^y \end{pmatrix} \quad (3b)$$

where  $( )^T$  indicates the transpose of a matrix. Note that the fixed nodes include the loaded nodes for which the locations are fixed in the process of optimization. Therefore,  $\mathbf{p}_{\text{fix}}^x$  includes the nodal loads and reactions at supports, and no loads are applied to the free nodes. It is seen from (3a) and (3b) that the  $x$ - and  $y$ -coordinates of free nodes and reactions are simply scaled by  $\alpha$  if the coordinates of fixed nodes and loads are scaled by  $\alpha$  in  $x$ - and  $y$ -directions, respectively, without changing the force densities of members. See Zhang and Ohsaki [9] for details.

It is known that the absolute values of stresses of existing members of the optimal solution take the same value, which is denoted by  $\bar{\sigma}$ , because the optimal truss under single loading condition is statically determinate and all members are fully stressed [10]. Although details are

not explained here, Ohsaki and Hayashi [7] showed that the minimization problem of compliance under volume constraint can be formulated as the minimization problem of the following objective function with respect to the force density only:

$$F(\mathbf{q}) = \sum_{i=1}^m \frac{\bar{\sigma}(L_i(\mathbf{q}))^2 |q_i|}{E} \quad (4)$$

where  $E$  is Young's modulus, and  $L_i$  is a function of the force density vector  $\mathbf{q}$  through the nodal coordinates obtained from (3a) and (3b). The volume constraint is satisfied with equality by adjusting the stress level  $\bar{\sigma}$ , and the cross-sectional area  $A_i$  of member  $i$  is obtained from  $L_i$ ,  $q_i$ , and  $\bar{\sigma}$  using (1) as

$$A_i = \frac{L_i |q_i|}{\bar{\sigma}} \quad (5)$$

### 3 Multiobjective optimization problem

Suppose the  $i$ th member is connected to two nodes  $i_1$  and  $i_2$ . Then,  $L_i^2$  is divided into the components of  $x$ - and  $y$ -coordinates as

$$L_i^2 = (x_{i_2} - x_{i_1})^2 + (y_{i_2} - y_{i_1})^2 \quad (6)$$

Using this relation, the objective function (4) is divided into two components as

$$F(\mathbf{q}) = F_x(\mathbf{q}) + F_y(\mathbf{q}) \quad (7)$$

where

$$F_x(\mathbf{q}) = \sum_{i=1}^m \frac{\bar{\sigma}}{E} (x_{i_2} - x_{i_1})^2 |q_i| \quad (8a)$$

$$F_y(\mathbf{q}) = \sum_{i=1}^m \frac{\bar{\sigma}}{E} (y_{i_2} - y_{i_1})^2 |q_i| \quad (8b)$$

Although it is not possible to actually divide the strain energy into the components of coordinates,  $F_x$  and  $F_y$  are regarded as  $x$ - and  $y$ -components of the strain energy, respectively. However, it should be noted that these components are different from those of compliance which is obtained by summation of the work done by each component of the external loads. Therefore, for example,  $F_x$  may have a non-zero value even when no load is applied in  $x$ -direction.

Note that the axial forces computed from  $\mathbf{q}$  and the nodal coordinates obtained from (3a) and (3b) do not satisfy equilibrium at the loaded nodes, because the loads are obtained as reactions at the fixed nodes, and they are not equal to the applied loads. In the formulation by Ohsaki and Hayashi [7], constraints are given for the equilibrium of the member forces with the applied loads. However, in this paper, the force density vector  $\tilde{\mathbf{q}}$  satisfying equilibrium conditions are recalculated, as follows, as a function of  $\mathbf{q}$  at each step of optimization because it is difficult to satisfy the equality constraints accurately when a genetic algorithm is used for optimization in the numerical example:

1. Assign  $\mathbf{x}_{\text{fix}}$ ,  $\mathbf{y}_{\text{fix}}$ , and  $\mathbf{q}$ .
2. Compute  $\mathbf{x}_{\text{free}}$  and  $\mathbf{y}_{\text{free}}$  by solving (3a) and (3b), respectively.
3. Compute  $L_i$  from the nodal coordinates and the cross-sectional area  $A_i = L_i |q_i| / \bar{\sigma}$  to obtain the stiffness matrix by incorporating displacement boundary conditions; i.e., the displacements are not fixed at the loaded nodes, although locations of loaded nodes are fixed for optimization.

4. Solve the stiffness equation to obtain the axial force  $\tilde{N}_i$ , and accordingly, the updated force density  $\tilde{q}_i = \tilde{N}_i/A_i$  that is regarded as a function of  $\mathbf{q}$ .

Accordingly,  $\mathbf{q}$  is an auxiliary variable vector that does not represent the true force densities. A multiobjective optimization problem is formulated, as follows, to minimize  $\tilde{F}_x(\mathbf{q}) = F_x(\tilde{\mathbf{q}}(\mathbf{q}))$  and  $\tilde{F}_y(\mathbf{q}) = F_y(\tilde{\mathbf{q}}(\mathbf{q}))$  under the bound constraints of  $\mathbf{q}$ :

$$\text{Minimize } \tilde{F}_x(\mathbf{q}) \text{ and } \tilde{F}_y(\mathbf{q}) \quad (9a)$$

$$\text{subject to } q_i^L \leq q_i \leq q_i^U \quad (i = 1, \dots, m) \quad (9b)$$

where  $q_i^U$  and  $q_i^L$  are the upper and lower bounds of  $q_i$ , respectively.

In the following numerical examples, Pareto optimal solutions of Problem (9) are generated simultaneously through a single optimization process using a multiobjective genetic algorithm. The problem is also solved using the linear weighted sum approach for comparison purpose. The objective function  $F^*(\mathbf{q})$  is formulated using nonnegative weight coefficients  $\mu_x$  and  $\mu_y$  as

$$\begin{aligned} F^*(\mathbf{q}) &= \mu_x \tilde{F}_x(\mathbf{q}) + \mu_y \tilde{F}_y(\mathbf{q}) \\ &= \sum_{i=1}^m \frac{\bar{\sigma}}{E} [\mu_x (x_{i2} - x_{i1})^2 + \mu_y (y_{i2} - y_{i1})^2] \sqrt{q_i^2 + c} \end{aligned} \quad (10)$$

where  $c$  is a small positive value for smoothing the function of absolute value for the optimization process using a nonlinear programming approach.

By comparing  $F^*(\mathbf{q})$  in (10) and  $F(\mathbf{q})$  in (4) with the relation (6), we can see that the optimal solution of a truss after scaling the locations of the supports and the loaded nodes in the initial ground structure by the factors  $\sqrt{\mu_x}$  and  $\sqrt{\mu_y}$ , respectively, in  $x$ - and  $y$ -directions is found by minimizing  $F^*(\mathbf{q}) = \mu_x \tilde{F}_x(\mathbf{q}) + \mu_y \tilde{F}_y(\mathbf{q})$ . Thus, the optimal solutions of the trusses with various aspect ratios can be found by solving a multiobjective optimization problem of minimizing  $\tilde{F}_x(\mathbf{q})$  and  $\tilde{F}_y(\mathbf{q})$  only once using an appropriate method, e.g., multiobjective genetic algorithm that can generate the set of Pareto optimal solutions with single process of optimization.

## 4 Numerical examples

Optimal shapes and topologies are found for a  $3 \times 2$  grid truss as shown in Fig. 1 as the initial ground structure, where a unit load is applied in negative  $y$ -direction at node 10. Note that the crossing diagonal members are not connected at their centers, and accordingly, the total number of members is 29. The scale in  $x$ - and  $y$ -directions are varied with the scales  $\sqrt{\mu_x}$  and  $\sqrt{\mu_y}$ , respectively, i.e.,  $H$  and  $W$  in Fig. 1 are scaled to  $\mu_x W$  and  $\mu_y H$ , respectively. In the following, ratio  $r = \sqrt{\mu_x/\mu_y}$  is taken as a parameter.

Pareto optimal solutions are found using the non-dominated sorting genetic algorithm (NSGA-III) implemented in the Python library DEAP Ver. 1.3.1 [11]. The numbers of population and generations are 40 and 500, respectively, and the probabilities of crossover and mutation are 0.9 and 0.0345 ( $= 1/m$ ), respectively. Young's modulus is  $E = 1.0$ . The stress of the existing members is tentatively set as  $\bar{\sigma} = 1.0$ , and the cross-sectional areas are uniformly scaled to have the specified total structural volume of 100 after obtaining the Pareto optimal solutions. Note that the units are omitted because they are not important.

Each individual is coded using real numbers  $q_i$  ( $i = 1, \dots, m$ ) as variables. Let  $q_{i0}$  denote the force density of the  $i$ th member of the ground structure in Fig. 1 with uniform cross-section. In the initial population, individuals are generated randomly in the range

$$q_{i0} - 10 \leq q_i \leq q_{i0} + 10 \quad (11)$$

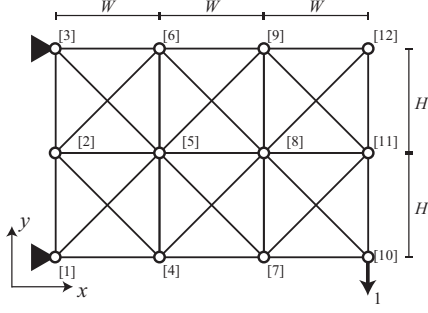


Figure 1:  $3 \times 2$  grid truss.

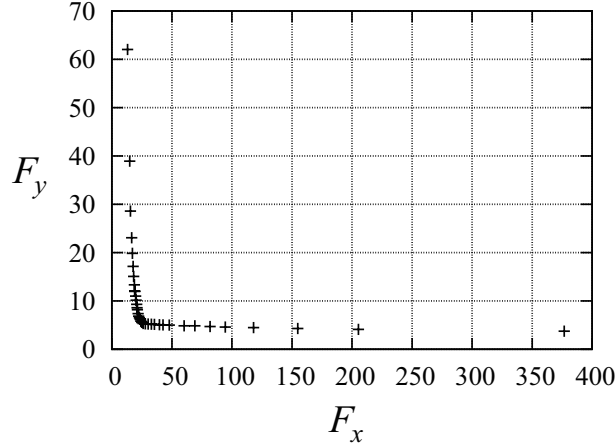


Figure 2: Pareto optimal solutions in the objective function space  $(F_x, F_y)$ .

After generating the Pareto front obtained using NSGA-III, the weight coefficients for each solution are approximately computed using the slope of the tangent line of the Pareto front in the objective function space. Let  $\mathbf{S}_i = (F_{xi}, F_{yi})$  denote the location of the  $i$ th Pareto optimal solution aligned in the increasing order of  $F_x$  on the  $(F_x, F_y)$  plane. The slope of the line connecting  $\mathbf{S}_i$  and  $\mathbf{S}_{i-1}$  is denoted by  $\beta_i$ , i.e.,

$$\beta_i = \frac{F_{yi} - F_{y(i-1)}}{F_{xi} - F_{x(i-1)}} \quad (12)$$

Then the ratio between the weight coefficients  $\mu_{xi}$  and  $\mu_{yi}$  for the  $i$ th solution is chosen from the range between  $\beta_{i+1}$  and  $\beta_i$  to estimate the value  $r_i = \sqrt{\mu_{xi}/\mu_{yi}}$ .

To compare the solutions to those obtained by NSGA-III, the sequential quadratic programming in the library SNOPT Ver. 7 [12] is used for minimizing the weighted sum of the objective functions  $F^*(\mathbf{q})$  in (10) with the smoothing parameter  $c = 1.0 \times 10^{-10}$ . Both for the genetic algorithm and linear weighted sum approach, the lower and upper bounds for  $q_i$  are given as  $q_i^L = -1000$  and  $q_i^U = 1000$ , respectively, which have sufficiently large absolute values not to restrict the solution space. Three individuals are generated by assigning three different sets of weight coefficients corresponding to  $r = 1.0, 2.0,$  and  $3.0$  for the linear weighted sum approach, and they are added to the initial population of NSGA-III to enhance diversity of the Pareto optimal solutions.

The '+' marks in Fig. 2 are the Pareto optimal solutions obtained by NSGA-III in the objective function space, where the solutions outside of the ranges of this figure are excluded. Note that optimization using NSGA-III has been carried out ten times from different initial solutions. The numbers of Pareto optimal solutions are 40, which is equal to the number of

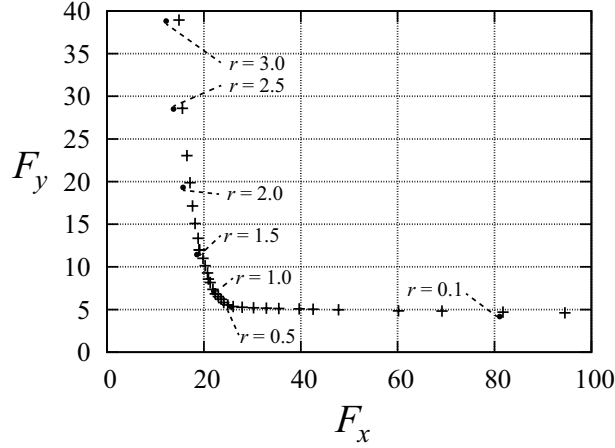


Figure 3: Pareto optimal solutions in the objective function space  $(F_x, F_y)$ ; ‘+’: solutions by NSGA-III, dots: solutions of Problem (9).

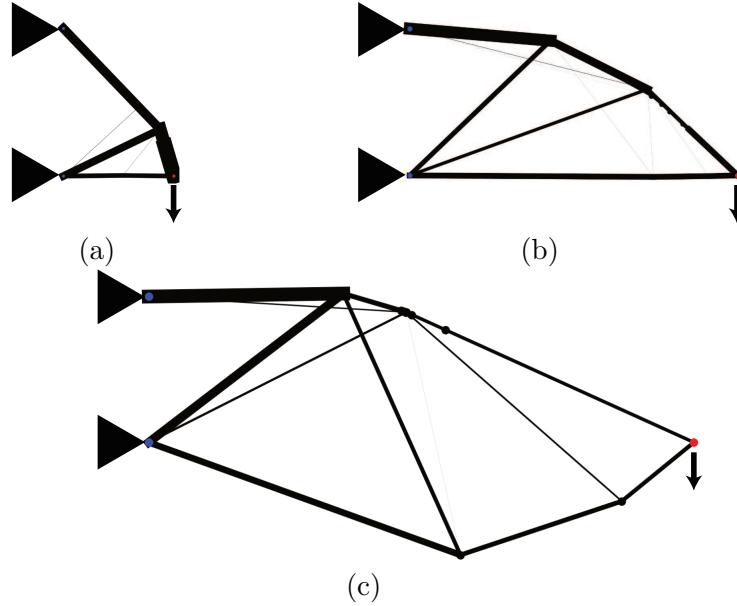


Figure 4: Optimal solutions: (a)  $r = 0.5$ , (b)  $r = 1.5$ , (c)  $r = 2.5$ .

population, for all cases. Fig. 2 shows the best case in view of diversity of solutions. It is seen from Fig. 2 that sufficiently large number of solutions are obtained, and the solutions are located along a convex curve in the objective function space. Figure 3 shows the Pareto optimal solutions in a smaller range of objective function space, where the optimal solutions obtained by the weighted sum approach are also plotted with dots and the corresponding  $r$  values. It is seen from the figure that the objective functions obtained by NSGA-III are slightly larger for a large value of  $r$ ; however, a good agreement in the objective values has been observed. The solutions obtained by NSGA-III for  $r = 0.5, 1.5, 2.5$  are shown in Figs. 4(a), (b), (c), respectively, with the same span in  $y$ -direction after scaling the nodal coordinates by 0.5, 1.5, and 2.5 in  $x$ -direction. Note that the width of each member is proportional to its cross-sectional area after scaling the ground structure to have the total structural volume of 100.

Table 1 shows the optimal compliance values obtained by the three different methods, where ‘Scaling’ refers to the solution obtained after actually scaling in  $x$ -direction by the ratio  $r$  and solving the single-objective optimization problem using the method by Ohsaki and Hayashi [7].

Table 1: Optimal compliance values obtained by three different methods.

Method	$r = 0.5$	$r = 1.5$	$r = 2.5$
Scaling	1.38	31.53	155.10
Weighted sum	1.46	31.78	151.29
NSGA-III	1.39	31.38	158.28

A good agreement is confirmed in Table 1, although inaccuracy in the  $r$  value for NSGA-III estimated from the slope of Pareto front is also regarded as a source of difference among the compliance values obtained by the three methods.

## 5 Conclusions

A new method of simultaneous optimization of geometry and topology has been presented for plane trusses to minimize the compliance under constraint on the total structural volume. Using the proposed method, the optimal shape and topology of trusses for various aspect ratios of the initial ground structure can be obtained as a set of Pareto optimal solutions through a single optimization process of a multiobjective genetic algorithm. The ratio between the weight coefficients for the two components of strain energy is obtained from the slope of the objective function values of the Pareto front in the objective function space. The ratio of scaling factors in the two directions of the ground structure is computed as the square root of the ratio of weight coefficients. It has been confirmed in the numerical example that the solutions corresponding to various aspect ratios of the initial ground structure are obtained with good accuracy in comparison to the solutions obtained by the weighted sum approach that demands solving an optimization problem for each aspect ratio of the ground structure.

## References

- [1] M. Ohsaki, Simultaneous optimization of topology and geometry of a regular plane truss, *Comput. & Struct.*, Vol. 66, pp. 69–77, 1998.
- [2] W. Achtziger, On simultaneous optimization of truss geometry and topology, *Struct. Multidisc. Optim.*, Vol. 33, 285–304, 2007.
- [3] B. Descamps and R. Coelho, The nominal force method for truss geometry optimization incorporating stability considerations, *Int. J. Solids Struct.*, Vol. 51, pp. 2390–2399, 2014.
- [4] A. Weldeyesus, J. Gondzio, L. He, M. Gilbert, P. Shepherd and A. Tyas, Truss geometry and topology optimization with global stability constraints, *Struct. Multidisc. Optim.*, Vol. 62, pp. 1721–1737, 2020.
- [5] H.-J. Schek, The force density method for form finding and computation of general networks, *Comp. Meth. Appl. Mech. Eng.*, Vol. 3, pp. 115 – 134, 1974.
- [6] B. Descamps, R. Coelho, L. Ney and P. Bouillard, Multicriteria optimization of lightweight bridge structures with a constrained force density method, *Comput. & Struct.*, Vol. 89, pp. 277–284, 2011.
- [7] M. Ohsaki and K. Hayashi, Force density method for simultaneous optimization of geometry and topology of trusses, *Struct. Multidisc. Optim.*, Vol. 56, 1157–1168, 2017.

- [8] W. Shen and M. Ohsaki, Geometry and topology optimization of plane frames for compliance minimization using force density method for geometry model, *Engineering with Computers*, Vol. 37, pp. 2029-2046, 2021.
- [9] J. Y. Zhang and M. Ohsaki, Stability conditions for tensegrity structures, *Int. J. Solids Struct.*, Vol. 44, pp. 3875–3886, 2007.
- [10] W. S. Hemp, *Optimum Structures*, Clarendon Press, 1973.
- [11] F.-A. Fortin, F.-M. De Rainville, M.-A. Gardner, M. Parizeau and C. Gagné, DEAP: Evolutionary algorithms made easy, *J. Machine Learning Research*, Vol. 13, pp. 2171–2175, 2012.
- [12] P. E. Gill, W. Murray and M. A. Saunders, SNOPT: An SQP algorithm for large-scale constrained optimization, *SIAM J. Opt.*, Vol. 12, pp. 979–1006, 1997.